

LOCAL MULTILAYER ANALYTIC SENSING FOR EEG SOURCE LOCALIZATION: PERFORMANCE BOUNDS AND EXPERIMENTAL RESULTS

D. Kandaswamy^{1,2}, T. Blu³, L. Spinelli⁴, C. Michel⁴ and D. Van De Ville^{1,2}

¹ Medical Image Processing Laboratory, Ecole Polytechnique Fédérale de Lausanne, CH-1015 Lausanne

² Medical Image Processing Laboratory, University of Geneva, CH-1211 Geneva

³ Department of Electronic Engineering, Chinese University of Hong Kong, Shatin N.T. Hong Kong

⁴ Functional Brain Mapping Group, University of Geneva, CH-1211 Geneva

ABSTRACT

Analytic sensing is a new mathematical framework to estimate the parameters of a multi-dipole source model from boundary measurements. The method deploys two working principles. First, the sensing principle relates the boundary measurements to the volumetric interactions of the sources with the so-called “analytic sensor,” a test function that is concentrated around a singular point outside the domain of interest. Second, the annihilation principle allows retrieving the projection of the dipoles’ positions in a single shot by polynomial root finding. Here, we propose to apply analytic sensing in a local way; i.e., the poles are not surrounding the complete domain. By combining two local projections of the (nearby) dipolar sources, we are able to reconstruct the full 3-D information. We demonstrate the feasibility of the proposed approach for both synthetic and experimental data, together with the theoretical lower bounds of the localization error.

Index Terms— EEG, source localization, finite rate of innovation, annihilating filter, dipole models, analytic functions

1. INTRODUCTION

Imaging the functioning of the human brain is an important task in neurosciences and neurology. To access the temporal properties of the brain circuits, electro- and magnetoencephalography (EEG, MEG) are predominant since they allow measuring signals down to millisecond resolution. Mapping back the measured signal $V|_{\partial\Omega}$ on the scalp surface $\partial\Omega$ to the source configuration ρ inside the brain is known as “source imaging” [1, 11]. Unfortunately, the underlying electromagnetic inverse problem is ill posed; i.e., an infinity of different source configurations can explain

the same scalp potential. Therefore, additional assumptions are required to make the solution unique. For this purpose, the various methods available are putting forward different hypotheses about the source model, which can be a single (equivalent) dipole [14, 16], multi-dipole [8, 9], or distributed dipoles [5, 10, 12]. In the latter case, the problem is underdetermined since the number of parameters of the model exceeds the number of measurements. Therefore, additional assumptions on the source distribution (e.g., smoothness, sparsity) needs to be taken into account.

In this paper, we focus on the multi-dipole source model, which is overdetermined but challenging since numerical optimization is trapped in local minima of the data fitting criterion. Interestingly, multi-dipole source localization received renewed interest from the mathematical community. In particular, Baratchart et al, proposed to solve the inverse problem analytically by so-called “best meromorphic approximation” [6, 7]. However, its extension to 3D requires an iterative process and the going through many 2D localizations. We propose to further extend the framework of analytic sensing to the 3-D multilayer setting. Analytic sensing relies on well-localized test functions, called analytic sensors, to retrieve information about the sources from boundary measurements [3]. It also uses the “finite rate of innovation” principle to solve the localization of the generating sources [18]. One property of 3-D application of analytic sensing is that we only recover a 2-D projection of the 3-D sources. Here, we only put analytic sensors (or, more correctly, their singular points or poles) near the locations where dipolar sources are expected. The method can be applied in a semi-automatic way (e.g., operator knows where to look for interesting generating sources) or in an automatic way (e.g., scanning the boundary with the “searchlight”).

The paper is organized as follows. In Sect. 2, we introduce the problem setting. In Sect. 3.1, we summarize the 2-D analytic sensing approach and extend the 2-D method to 3-D. In sect. 4, we compare the precision of our reconstruction algorithm against the Cramér-Rao Lower Bounds (CRLBs). Finally, we use our approach to localize sources for experi-

This work was supported by the Swiss National Science Foundation (grant 200021-119812), the Sino Swiss Science and Technology Cooperation Program (EG03-092008), and by the Center for Biomedical Imaging of the Geneva-Lausanne Universities and the EPFL, as well as the foundations Leenaards and Louis-Jeantet and The Microsoft-Chinese University-Joint Laboratory Research student grant.

mental EEG in a somatosensory stimulus and compare the obtained result with those obtained by LAURA [13].

2. PROBLEM FORMULATION

In EEG, one measures the electrical potential V on the scalp surface $\partial\Omega$. These potential differences are the manifestation of a source distribution ρ in the brain, which is governed by the equation:

$$-\nabla \cdot (\sigma \nabla V) = \rho, \quad (1)$$

where σ is the conductivity of the head. A popular head model is the multi-shell spherical head model with piecewise constant conductivities [15]. Since no current can leave the head, we also have the following boundary condition:

$$(\nabla V)|_{\partial\Omega} \cdot \mathbf{e}_\Omega = 0, \quad (2)$$

where \mathbf{e}_Ω is the outward surface normal. The problem at hand, which is the inverse problem associated to EEG, can be described as:

from $V|_{\partial\Omega}$, reconstruct ρ .

However, this inverse problem is ill-posed as the solution is non-unique and hence, we need additional constraints. Here, we restrict ρ to a parametric source model, more specifically the multi-dipole model which can be written as:

$$\rho(\mathbf{x}) = \sum_{k=1}^K \mathbf{p}_k \cdot \nabla \delta(\mathbf{x} - \mathbf{x}_k), \quad (3)$$

where we have $6K$ unknowns; i.e., the dipoles' positions $\mathbf{x}_k = [x_k \ y_k \ z_k]^T$ and moments $\mathbf{p}_k = [p_{k1} \ p_{k2} \ p_{k3}]^T$.

3. LOCAL MULTILAYER ANALYTIC SENSING

3.1. Source Localization in 3D

Sensing Principle: We consider a closed 3-D region Ω with piecewise constant conductivity σ . Then, Poisson's equation, $-\nabla \cdot (\sigma \nabla V) = \rho$, holds within Ω . Applying Green's theorem yields the following surface integral:

$$\langle \psi, \rho \rangle = - \oint_{\partial\Omega} V \nabla \psi \cdot \mathbf{e}_\Omega \, ds, \quad (4)$$

where we have taken into account the boundary condition (2). Moreover, ψ is a special function called "multilayer analytic sensor", chosen such that $\nabla \cdot (\sigma \nabla \psi)|_\Omega = 0$. In [4], we give the expression of the analytic sensor $\psi_{a_n}(x, y, z)$ in such a way that it coincides with the analytic function $\ln(x + iy - a_n)$ in the inner compartment (the brain) where the sources are supposed to be. We need the analytic sensor's singular point $a_n = \alpha \exp(in\theta)$ to be outside Ω . Therefore, using a set of analytic sensors, we can compute generalized measures containing information on ρ knowing only $V|_{\partial\Omega}$.

Annihilation Principle: The main principle behind our technique is that the dipole positions $\mathbf{x}_k = [x_k \ y_k]^T$ can be found as the complex roots $x_k + iy_k$ of a polynomial of degree K . In particular, under the assumption of the source model, the generalized measures should equal

$$\langle \psi_{a_n}, \rho \rangle = \sum_{k=1}^K \frac{p_{k1} + ip_{k2}}{x_k + iy_k - a_n}, \quad (5)$$

which can be rephrased under the form $\sum_{k=0}^{K-1} c'_k e^{ink\theta} / R(a_n)$, $c'_k \in \mathbb{R}$, with $R(X) = \sum_{k=0}^K r_k X^k$ a polynomial of degree K with roots $x_k + iy_k$. The key observation is that the numerator $\sum_{k=1}^{K-1} c'_k e^{ink\theta}$ can be annihilated by a filter h with \mathcal{Z} -transform

$$H(z) = \sum_{k \in \mathbb{Z}} h_k z^{-k} = \prod_{k=0}^{K-1} (1 - e^{ik\theta} z^{-1}). \quad (6)$$

Therefore, we have that

$$h_n * (R(a_n) \langle \psi_{a_n}, \rho \rangle) = 0 \quad (7)$$

holds, which is a linear system of equations in r_k . Solving (7) determines the polynomial R , and the dipole positions from its roots. The dipole moments $\mathbf{p}_k = [p_{k1} \ p_{k2}]^T$ are obtained by solving a linear system of equations (5) with known $x_k + iy_k$. For an in-depth explanation, we refer to [3].

3.2. Local Analytic Sensing in 3-D

The annihilation principle allows recovering a projection of \mathbf{x}_k on the X-Y plane. Hence, if we introduce a coordinate transform:

$$\begin{bmatrix} x' \\ y' \end{bmatrix} = \begin{bmatrix} 1 & 0 & 0 \\ 0 & 1 & 0 \end{bmatrix} \mathbf{R} \begin{bmatrix} x \\ y \\ z \end{bmatrix}, \quad (8)$$

with \mathbf{R} some rotation matrix, then the corresponding analytic sensor restricted to the inner compartment, i.e., the brain, reads as:

$$\psi_{a_n}(x', y') = \ln(x' + iy' - a_n), \quad a_n \notin \Omega. \quad (9)$$

When applying the FRI approach to retrieve the dipoles' locations we retrieve

$$\begin{bmatrix} x'_k \\ y'_k \end{bmatrix}^T = \begin{bmatrix} 1 & 0 & 0 \\ 0 & 1 & 0 \end{bmatrix} \mathbf{R} \begin{bmatrix} x_k \\ y_k \\ z_k \end{bmatrix}.$$

If we define a set of such rotation matrices \mathbf{R}_j , $j = 1 \dots L$, then we obtain a set of 2-D projections $\{x'_k + iy'_k\}_{j=1 \dots L}$ of the locations \mathbf{x}_k . Thus, fully recovering \mathbf{x}_k boils down to reconstructing a 3-D vector from its 2-D projections which is a well-studied and well-understood problem [2].

Another key property of this reconstruction scheme is that the analytic sensors are well-localized around $a_n =$

$\alpha \exp(in\theta)$, as illustrated in Fig. 1. We do need a number of sensors with poles a_n , $n = 0, \dots, N - 1$, but not necessarily surrounding the domain Ω . Consequently, we can put sensors only locally, which ignores distant dipoles. Such prior knowledge improves the assumption that a limited number of dipoles needs to be localized. The concept of local analytic sensing is illustrated in Fig. 3(b); i.e., the large black dots are poles of the analytic sensors (in two planes).

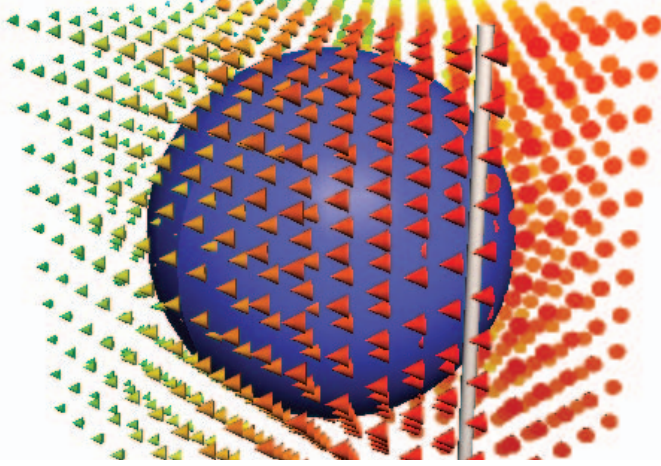


Fig. 1. The analytic sensor $\psi_{a_n}(\mathbf{x})$, with pole $a_n = 1.01$. Color and size of the arrows represent the magnitude of the analytic sensor; their directions the complex argument.

4. EXPERIMENTAL RESULTS

In this section, we show the feasibility of the multi-planar analytic sensing technique with both synthetic and experimental data. We use a 3-shell conductor model, as depicted in figure 2. Such a model is used in the SMAC head model [15], where the compartments represent the brain, skull and scalp with radii $r_1 = 0.88, r_2 = 0.9350$ and $r_3 = 1$ and corresponding conductivities $\sigma_1 = 1, \sigma_2 = 0.0125$ and $\sigma_3 = 1$.

4.1. Synthetic data

To evaluate the performance of the proposed algorithm in the presence of noise, we compute the Cramér-Rao lower bounds (CRLBs) for an EEG setting with the additive white Gaussian noise hypothesis [17]. That is, given an electrode cap, these bounds establish the minimal covariance matrix of any unbiased estimate of the position and moment parameters.

The signal model describing the noisy potential measures, $\tilde{v}(\mathbf{x}; \mathbf{e}_n)$, is the following:

$$\tilde{v}(\boldsymbol{\theta}; \mathbf{e}_n) = v(\boldsymbol{\theta}; \mathbf{e}_n) + \varepsilon_n, \quad (10)$$

where $v(\boldsymbol{\theta}; \mathbf{e}_n)$ is the theoretical potential difference measured at electrode $\mathbf{e}_n, \boldsymbol{\theta} = [\mathbf{x}_1, \mathbf{p}_1, \dots, \mathbf{x}_M, \mathbf{p}_M]$ the source

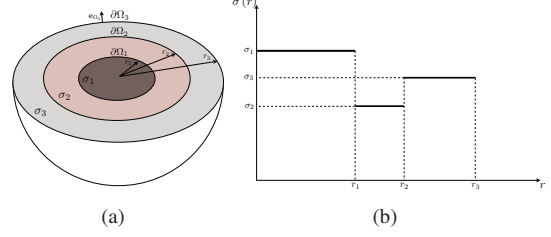


Fig. 2. Figure 2(a) depicts a 3-sphere conductor model. Each compartment, Ω_i , has its own characteristic conductivity, σ_i for $i \in \{1, \dots, 3\}$. Figure 2(b) depicts the corresponding conductivity profile as a function of r (which is in this case a piecewise constant). Each discontinuity represents a boundary $\partial\Omega_1, \partial\Omega_2$ or $\partial\Omega_3$.

model's parameters and ε_n a normally distributed random variable with expected value 0 and variance σ^2 .

In order to compute these lower bounds, we determine the Fisher information matrix, $\mathbf{J} = [J_{k,l}]_{k,l \in \{1, \dots, 6M\}}$, corresponding to (10), which reads as follows:

$$J_{k,l} = \frac{1}{\sigma^2} \sum_{n=1}^P \frac{\partial}{\partial \theta_k} v(\boldsymbol{\theta}; \mathbf{e}_n) \frac{\partial}{\partial \theta_l} v(\boldsymbol{\theta}; \mathbf{e}_n), \quad (11)$$

with P the number of electrodes. The Cramér-Rao bounds are the diagonal elements of \mathbf{J}^{-1} . The most important aspect when performing source localization (e.g., in partial epilepsy) is the reconstruction of the location parameters \mathbf{x}_m . Hence, when simulating we only consider the estimation of the location parameters.

Figure 3(a) depict the setup, i.e., the SMAC head model and corresponding electrodes and the generating dipole whereas figure 3(b) depicts the generated boundary potential and the positions of the singularities a_n . We added noise to the measured potential and plotted the lower bound on the localization error, $\epsilon = \sqrt{\sigma_x^2 + \sigma_y^2 + \sigma_z^2}$ (where σ_x^2, σ_y^2 and σ_z^2 are the CRLBs in X, Y and Z), and the obtained localization errors against the corresponding noise level in figure 4.1. We see that we are rather close to the CRLBs. However we would like to point out that for high SNRs our method will not perform as well as the CRLBs might indicate because of the integral (4). That is, this integral requires that we know $V|_{\partial\Omega}$. Since we have V only at the electrode sites we need an interpolation/approximation scheme which renders the computation of the generalized samples erroneous even when the measured signal is of high quality. Hence, further research to devise a proper interpolation/approximation approach could potentially be fruitful. Note that, in reality the measured signal is of rather low quality.

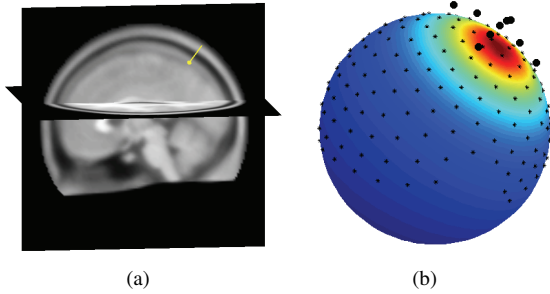


Fig. 3. Figure 3(a) depicts the SMAC head model, the electrodes (represented by the black dots) and the generating dipole (depicted in red). This dipole is a radial unit dipole located at $\mathbf{x}_1 = [-0.4 \ 0.2 \ 0.6]^T$. Figure 3(b) depicts the noiseless generated boundary potential and the placements of the singularities a_n (the black dots).

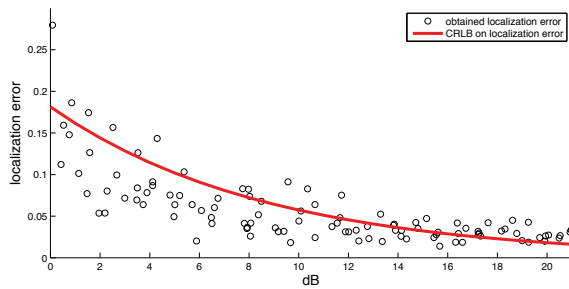


Fig. 4. This figure plots the expected minimal localization error made by any unbiased estimator, in red, against the signal-to-noise-ratio (SNR). The black dots show the localization errors made by our reconstruction algorithm for an instance of a noisy set of EEG measurements at a given SNR.

4.2. Experimental Data

Two stimulus evoked data sets were collected from normal, healthy research subjects using a 204-channel EEG system. The first data set is a sensory evoked potential (SEP) paradigm, where the subject’s left index finger was tapped for a total of 100 trials. The second data set is a SEP paradigm as well, but the subject’s right index finger was tapped for a total of 100 trials. The measured signals were then averaged over the number of trials to obtain a high quality signal. We localized a single dipole for each averaged signal, using our reconstruction algorithm (the assumption that the underlying source distribution can be modeled through a single dipole is a valid a priori for such paradigms). Figures 5(a) and 5(b) show the averaged signals when tapping the left index and right index finger. The vertical red line marks when the dipole model is most valid, i.e., 50 ms after the tap. The first row of Fig. 6 depicts the characteristic boundary potential of the SEP paradigm where the left finger is tapped and the corre-

sponding source localization, using our method whereas the second line depicts the characteristic boundary potential of the SEP paradigm where the right finger is taped and the corresponding source localization.

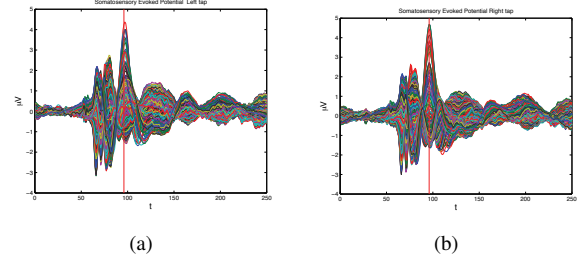


Fig. 5. Figures 5(a) and 5(b) depict the measured signals averaged over 1000 trials, when the subject is tapped on the left and right index finger, respectively. The vertical red line is placed 50 ms after the event (a tap on the left or right index finger). At this moment, the underlying source distribution ρ is well-modeled by a dipole model.

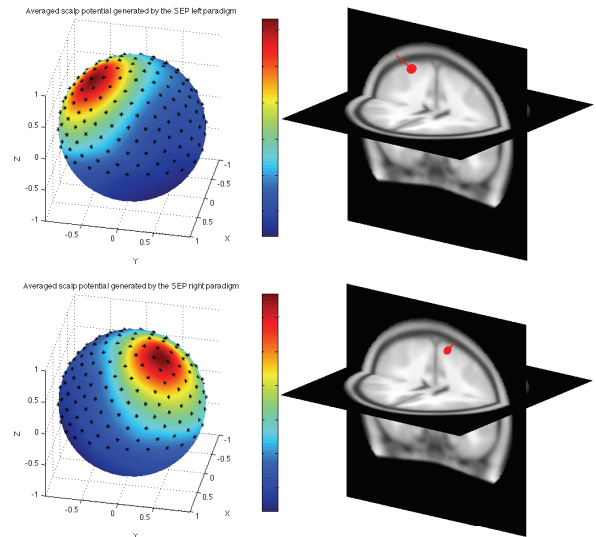


Fig. 6. The generated boundary potentials and their corresponding source localizations using local multilayer analytic sensing.

5. CONCLUSION, DISCUSSION & OUTLOOK

We proposed a new parametric approach to estimate dipolar sources from EEG measurements. The method has several attractive properties such as the ability to locally “sense” and localize the sources, which makes the multi-dipole assumption more reasonable. The preliminary results in this paper show that this method works appropriately for average evoked potentials. We are currently improving the visual representation

of our results so as to facilitate future comparisons with standard localization methods (e.g., LAURA, LORETA). Future work will focus on signals with low(er) signal-to-noise ratio and stimulation paradigms that evoke (known) multi-dipole configurations.

6. REFERENCES

- [1] S. Baillet, J. C. Mosher, and R. M. Leahy. Electromagnetic brain mapping. *IEEE Signal Processing Magazine*, 18(6):14–30, 2001.
- [2] Tomasi C and Kanade T. Shape and motion from image streams under orthography: a factorization method. *International Journal of Computer Vision*, 9(2):137–154, 1992.
- [3] Kandaswamy D, Blu T, and Van De Ville D. Analytic sensing: Noniterative retrieval of point sources from boundary measurements. *SIAM Journal on Scientific Computing*, 31:3179–3194, 2009.
- [4] Kandaswamy D, Blu T, and Van De Ville D. Source imaging using analytic sensing for multi-layer spherical models. *Physics in Medicine and Biology*, To be submitted.
- [5] Wipf D P, Owen J P, Attias H T, Sekihara K, and Nagarajan S S. Robust bayesian estimation of the location, orientation, and time course of multiple correlated neural sources using MEG. *Neuroimage*, 49(1):641–655, 2010.
- [6] Baratchart L, Ben Abda A, Ben Hassen F, and Leblong J. Recovery of pointwise sources or small inclusions in 2d domains and rational approximation. *Inverse problems*, 21:51–74, 2005.
- [7] Baratchart L, Leblond J, and Marmorat JP. Inverse sources problem in a 3d ball from best meromorphic approximation on 2d slices. *Electronic Transactions on Numerical Analysis*, 25:41–53, 2006.
- [8] Scherg M and von Cramon D. Two bilateral sources of the late aep as identified by a spatio-temporal dipole model. *Electroencephalogr Clin Neurophysiol*, 62:32–44, 1985.
- [9] Scherg M, Bast T, and Berg P. Multiple source analysis of interictal spikes: goals, requirements, and clinical value (review). *J Clin Neurophysiol*, 16:214–224, 1985.
- [10] Singh M, Doria D, Henderson V, Huth G, and Beatty J. Reconstruction of images from neuro-magnetic fields. *IEEE Trans Nucl Sci*, NS31:585–589, 1984.
- [11] C. M. Michel, M. M. Murray, G. Lantz, S. Gonzalez, L. Spinelli, and R. Grave de Peralta. EEG source imaging. *Clin Neurophysiol*, 115:2195–2222, 2004.
- [12] Grave de Peralta R, Murray MM, Michel CM, Martuzzi R, and Gonzalez Andino S. Electrical neuroimaging based on biophysical constraints. *Neuroimage*, 21:527–539, 2004.
- [13] Grave de Peralta R, Gonzalez S, Lantz G, CM Michel, and Landis T. Noninvasive localization of electromagnetic epileptic activity: I. method descriptions and simulations. *Brain Topogr*, 14:131–137, 2001.
- [14] P. Schimpf, C. Ramon, and J. Hauelsen. Dipole models for the EEG and MEG. *IEEE Transactions on Biomedical Engineering*, 49(5):409–418, 2002.
- [15] L. Spinelli, S. G. Andino, G. Lantz, M. Seeck, and C. M. Michel. Electromagnetic inverse solutions in anatomically constrained spherical head models. *Brain Topography*, 13:115–125, 2000.
- [16] C.J. Stok. The influence of model parameters on EEG/MEG single dipole source estimation. *IEEE Transactions on Biomedical Engineering*, 34(4):290–296, 1987.
- [17] Blu T, Dragotti P.L., Vetterli M., Marziliano P., and Coulot L. Sparse sampling of signal innovations. *IEEE Signal Processing Magazine*, 25(2):31–40, 2008.
- [18] M. Vetterli, P. Marziliano, and T. Blu. Sampling signals with finite rate of innovation. *IEEE Transactions on Signal Processing*, 50(6):1417–1428, 2002.